

# Ovatoxin-a, A Palytoxin Analogue Isolated from *Ostreopsis cf. ovata* Fukuyo: Cytotoxic Activity and ELISA Detection

Marco Pelin,<sup>†</sup> Martino Forino,<sup>‡</sup> Valentina Brovedani,<sup>†</sup> Luciana Tartaglione,<sup>‡</sup> Carmela Dell'Aversano,<sup>‡</sup> Rossella Pistocchi,<sup>§</sup> Mark Poli,<sup>#</sup> Silvio Sosa,<sup>†</sup> Chiara Florio,<sup>†</sup> Patrizia Ciminiello,<sup>‡</sup> and Aurelia Tubaro<sup>\*,†</sup>

<sup>†</sup>Department of Life Science, University of Trieste, 34127 Trieste, Italy

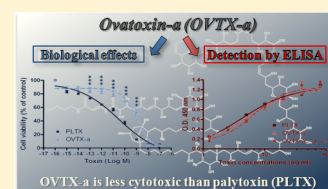
<sup>‡</sup>Department of Pharmacy, University of Napoli Federico II, 80131 Napoli, Italy

<sup>§</sup>Interdepartmental Center for Research in Environmental Sciences, University of Bologna, 481230 Ravenna, Italy

<sup>#</sup>U.S. Army Medical Research Institute of Infectious Diseases, Ft. Detrick, Maryland, 21701-5011 United States

## Supporting Information

**ABSTRACT:** This study provides the first evaluation of the cytotoxic effects of the recently identified palytoxin (PLTX) analog, ovatoxin-a (OVTX-a), the major toxin produced by *Ostreopsis cf. ovata* in the Mediterranean Sea. Its increasing detection during *Ostreopsis* blooms and in seafood highlights the need to characterize its toxic effects and to set up appropriate detection methods. OVTX-a is about 100 fold less potent than PLTX in reducing HaCaT cells viability ( $EC_{50} = 1.1 \times 10^{-9}$  M vs  $1.8 \times 10^{-11}$  M, MTT test) in agreement with a reduced binding affinity ( $K_d = 1.2 \times 10^{-9}$  vs  $2.7 \times 10^{-11}$  M, saturation experiments on intact cells). Similarly, OVTX-a hemolytic effect is lower than that of the reference PLTX compound. Ost-D shows the lowest cytotoxicity toward HaCaT keratinocytes, suggesting the lack of a hydroxyl group at C44 as a critical feature for PLTXs cytotoxic effects. A sandwich ELISA developed for PLTX detects also OVTX-a in a sensitive (LOD = 4.2 and LOQ = 5.6 ng/mL) and accurate manner (Bias = 0.3%), also in *O. cf. ovata* extracts and contaminated mussels. Although in vitro OVTX-a appears less toxic than PLTX, its cytotoxicity at nanomolar concentrations after short exposure time rises some concern for human health. The sandwich ELISA can be a viable screening method for OVTXs detection in monitoring program.



## INTRODUCTION

Palytoxin (PLTX) is a highly toxic marine compound originally isolated in 1971 from *Palythoa toxica* corals<sup>1,2</sup> and subsequently identified in *Ostreopsis* dinoflagellates<sup>3,4</sup> and *Trichodesmium* marine cyanobacteria.<sup>5</sup>

A series of PLTX analogues have been identified, so far. Among them, four analogues have been chemically and/or biologically characterized: (i) 42S-OH-50S-PLTX, isolated from *Palythoa toxica*,<sup>6</sup> which in acute oral toxicity studies in mice is comparable in potency to PLTX;<sup>7</sup> (ii) its stereoisomer due to a conformational inversion on C50 (42S-OH-50R-PLTX) extracted from *Palythoa tuberculosa*, whose cytotoxicity is 100 times lower than that of PLTX;<sup>8</sup> (iii) ostreocin-D (Ost-D), isolated from *Ostreopsis siamensis*, which appears less toxic than PLTX in vivo;<sup>9</sup> (iv) ovatoxin-a (OVTX-a), produced by *Ostreopsis cf. ovata* in the Mediterranean Sea (Figure 1).<sup>10</sup> Intriguingly, the Mediterranean *Ostreopsis cf. ovata* strain was found to produce OVTX-a as the major toxin, in addition to other OVTXs (OVTX-b to -h), and only low amounts of a putative PLTX<sup>10,11</sup> recently renamed isobaric PLTX.<sup>12</sup>

PLTX has been detected in different edible marine organisms, including fish, crustaceans, mollusks, and echinoderms. Consumption of PLTX-contaminated fish and crabs has been associated with human poisonings, with some fatal outcomes in tropical and subtropical areas.<sup>4</sup> On the contrary, in temperate areas such as the Mediterranean Sea, human adverse effects ascribed to PLTXs have been associated mainly

with cutaneous and inhalational exposure to aerosolized seawater during *Ostreopsis* blooms and with handling zoanthid corals in home aquaria. These problems, characterized mainly by dermatitis, respiratory distress, and fever, are far more frequent, but likely underestimated.<sup>4,13</sup> Intriguingly, OVTX-a seems to be the major toxin identified in *O. cf. ovata* in the Mediterranean area, so far. However, no human intoxications ascribed to these toxins have been documented in this area, despite the presence of high amounts of OVTX-a have been frequently detected in seafood.<sup>11,14,15</sup> This suggests a lower OVTX-a toxicity than that of the PLTX parent compound, although the knowledge on the toxic potential of OVTX-a is very scarce: the only available information derived from in vitro studies on *O. ovata* extracts containing OVTXs mixtures. In particular, the hemolytic activity of semipurified *O. cf. ovata* extracts was evaluated using sheep erythrocytes,<sup>11,16</sup> while Crinelli et al. showed an increased expression of genes encoding for inflammation-related proteins in human macrophages exposed to a semipurified extract.<sup>17</sup> Furthermore, uncharacterized *O. cf. ovata* extracts were shown to induce cytoskeletal disorganization, apoptosis, and dysregulation of gene expression in HeLa cells.<sup>18</sup> In addition, few studies highlighted a series of

Accepted: December 29, 2015

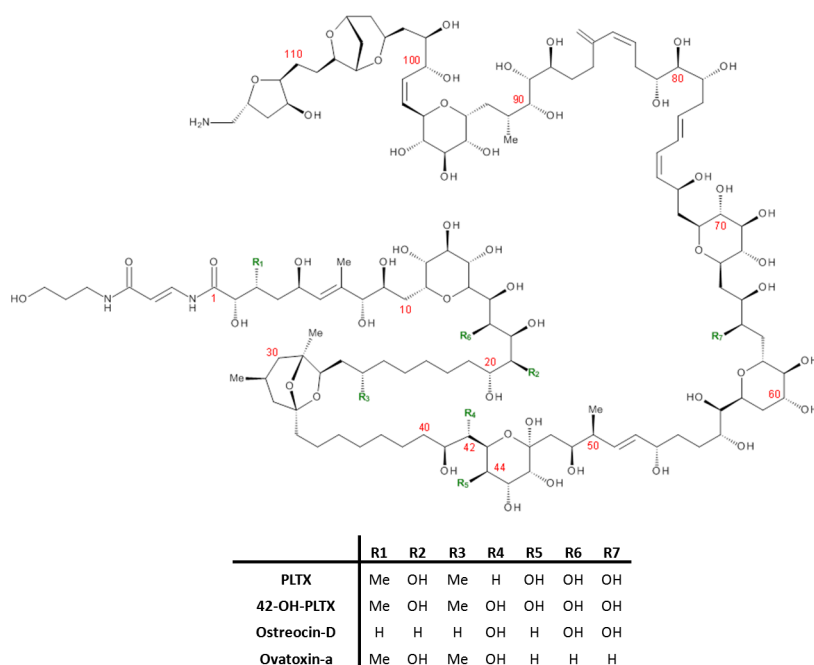


**Figure 1.** Molecular structure of PLTX and some analogues.

toxic effects for *O. cf. ovata* extracts on marine organisms, such as mussels,<sup>19</sup> crustaceans and fish,<sup>20</sup> and sea urchins.<sup>21</sup> Nevertheless, a complete characterization of OVTX-a adverse effects using predictive models of toxicity for humans is not available, so far.

Given the growing cases of adverse effects attributed to OVTXs detected in both *Ostreopsis* and marine aerosols in the Mediterranean Sea,<sup>22–26</sup> it is very important to define the toxicological profile of OVTX-a, and to develop a rapid detection method suitable for monitoring programs. Due to the limited availability of purified OVTX-a, an *in vitro* approach was used to investigate its toxic effects on skin HaCaT keratinocytes, whereas an immunoenzymatic assay set up for PLTX was evaluated for its ability to detect also OVTX-a.

## EXPERIMENTAL SECTION

**Toxins.** Palytoxin, isolated from *Palythoa tuberculosa*, was purchased from Wako Pure Chemical Industries Ltd. (Osaka, Japan; lot number WKL7151, purity >90%). A semipurified sample of OVTX-a at purity grade of 51% (Table S1) and a mixture of OVTXs, containing OVTX-a, -d, and -e, were isolated from cultures of Mediterranean strains of *O. cf. ovata* as previously described<sup>10</sup> and used for cytotoxicity assays.

Briefly, cell pellets ( $300 \times 10^6$  cells with a toxin content of 19 pg/cell) were extracted with MeOH/H<sub>2</sub>O (1:1, v/v) and partitioned with CH<sub>2</sub>Cl<sub>2</sub>. A crude extract containing 5.6 mg of OVTX-a was obtained, evaporated to dryness, and loaded onto a 360-g Combiflash C-18 column. The column was eluted with H<sub>2</sub>O:PrOH on a linear gradient from 60:40 to 10:90 over 50 min. Flow was 5 mL/min. A 75 mL fraction containing OVTXs was collected after 13 min, evaporated to dryness, and further separated on a Gemini 10  $\mu$ m high performance liquid chromatography (HPLC) column, 10  $\times$  200 mm (Phenomenex, Torrance, CA, USA) with a linear gradient of H<sub>2</sub>O–CH<sub>3</sub>CN–AcOH from 80:20:01 to 0:100:0.1 over 30 min. Final purification of OVTX-a was achieved on a Kinetex 2.6  $\mu$ m HPLC column, 4.6  $\times$  100 mm (Phenomenex, Torrance, CA, USA). This last purification was carried out by using a 20 min

gradient with the same mobile phases as above. In preparative HPLC, high resolution mass spectrometry (HRMS) detection was used splitting the flow before the ion source. OVTX-a (700  $\mu$ g, purity 51%) was isolated and the recovery of the entire isolation procedure was estimated to be 12.5%. Sample purity (%) was measured by liquid chromatography high-resolution mass spectrometry (LC-HRMS) in full MS positive ion mode using extracted ion chromatogram (XIC) areas.

Ost-D, used for structure–activity relationship analysis, was kindly provided by Prof. Yasumoto (Japan Food Research Laboratories) and extracted from *O. siamensis* collected along Aka Island (Okinawa, Japan) coasts as previously described.<sup>27</sup>

**Extraction of Naturally Contaminated *Ostreopsis cf. ovata* Cells and Mussels.** *O. cf. ovata* OOAN0816 strain was isolated by the capillary pipet method<sup>28</sup> from samples collected in 2008 in the Northern Adriatic Sea (Marche region, Italy) and deposited in the culture collection of University of Bologna (Ravenna campus, Italy). Cultures were maintained in natural seawater, at salinity of 36 ppt in modified *f/2* medium containing 5-fold diluted macronutrients and selenium, and kept in a thermostatic chamber at 20 °C, 16:8 h light–dark cycle and irradiance of 100–110  $\mu$ mol/m<sup>2</sup>/s from cool white lamps. Cells were then separated from culture media by gravity filtration and extracted three times with MeOH/H<sub>2</sub>O 1:1 obtaining an extract at a final concentration of 0.1 g/mL. Cell media were extracted by three repartitions with BuOH (*Ostreopsis* culture media) as previously described.<sup>29</sup>

Mussels (*Mytilus galloprovincialis*) edible parts were extracted three times with MeOH/H<sub>2</sub>O 8:2 obtaining an extract at a final concentration of 0.1 g/mL as previously described.<sup>29</sup>

These extracts were analyzed by the sandwich ELISA after 1:10 or 1:100 dilution in assay buffer to overcome matrix effect, and the results confirmed by LC-HRMS.

**Liquid Chromatography High-Resolution Mass Spectrometry Analyses.** LC-HRMS analyses were performed on a hybrid linear ion trap LTQ Orbitrap XL Fourier transform mass spectrometer (FTMS) with an ESI ION MAX source (Thermo-Fisher, USA) combined with an Agilent 1100 LC

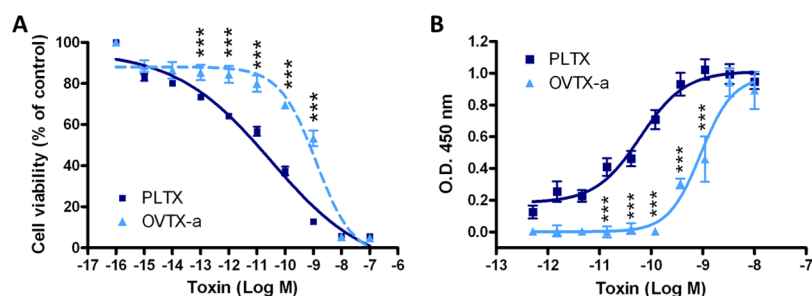


**Figure 2.** Effects of OVTX-a on HaCaT cells. (A) Cells were exposed to OVTX-a and PLTX ( $10^{-16}$ – $10^{-7}$  M) for 4 h and cell viability evaluated by MTT assay. Results are reported as % of control (untreated cells). (B) Specific binding of OVTX-a compared to that of PLTX; nonspecific bindings were obtained in the presence of  $1.0 \times 10^{-3}$  M OUA. Results are the means  $\pm$  SE of five different experiments performed in triplicate. Statistical differences: \*\*\*,  $p < 0.001$  (two-way ANOVA and Bonferroni's post test).

binary system (USA) according to Ciminiello et al.<sup>15</sup> A Kinetex C18, 2.6  $\mu$ m,  $2.10 \times 100$  mm (Phenomenex, USA) column was used. Mobile phase was A = H<sub>2</sub>O, 30 mM acetic acid, and B = MeCN/H<sub>2</sub>O (95:5), 30 mM acetic acid. Flow rate was 0.2 mL/min and injection volume 5  $\mu$ L. The following gradient elution was used: 25–30% B in 15 min; 30–100% B in 1 min; 100% B for 5 min. PLTX standard was used to generate a five-level calibration curve (25, 12.5, 6.25, 3.13, and 1.6 ng/mL). Calibration points were the result of triplicate injections, and peak areas were used for plotting. The curve was used to quantify positive samples assuming that OVTXs present the same molar response as PLTX. Under the described instrumental conditions, measured limit of detection (LOD) and quantitation (LOQ) for the PLTX standard was 1.6 ng/mL and 3.13 ng/mL.

**HaCaT Cells Culture.** HaCaT cell line was purchased from Cell Line Service (DKFZ, Eppelheim, Germany) and cultured in DMEM containing 10% fetal bovine serum (FBS),  $1.0 \times 10^{-2}$  M glutamine,  $1.0 \times 10^{-4}$  g/mL penicillin, and  $1.0 \times 10^{-4}$  g/mL streptomycin, at 37 °C in a humidified 95% air/5% CO<sub>2</sub> atmosphere. Cell passage was performed 2 days postconfluence, once per week. All of the experiments were performed between passage 50 and 65.

**MTT Assay.** Cells ( $3 \times 10^3$  cells/well) were seeded in 96-wells plates and, after 72 h, exposed to the toxins for 4 h. Cells were then washed, and fresh culture medium containing 3-(4,5-Dimethylthiazol-2-yl)-2,5-diphenyltetrazolium bromide (MTT, 0.5 mg/mL) was added. After 4 h, the insoluble crystals were solubilized in 200  $\mu$ L of DMSO/well, and the absorbance was measured by an Automated Microplate Reader EL 311s (Bio-Tek Instruments, Winooski, VT, USA) at 540/630 nm.

**Binding Assay.** Saturation experiments were performed on HaCaT cells ( $1 \times 10^4$ /well) as previously described.<sup>30</sup> Briefly, after 10 min exposure to PLTX or OVTX-a, cells were washed with Dulbecco's phosphate buffered saline (D-PBS), fixed with 4% paraformaldehyde (PFA) and blocked in TBB buffer (50 mM Tris-HCl, 0.15 M NaCl, 2% BSA, and 0.2% Tween 20, pH 7.5) containing 10% horse serum. Nonspecific binding was determined in the presence of  $1 \times 10^{-3}$  M ouabain (OUA). Toxin binding was detected by exposing the cells to 2  $\mu$ g/mL mouse anti-PLTX 73D3 monoclonal antibody (mAb) and 1:3000 HRP conjugated antimouse IgG (DakoCytomation; Milan, Italy) for 1 h at 37 °C each. After washing, the colorimetric reaction was started by adding 60  $\mu$ L of 3,3',5,5'-tetramethylbenzidine (TMB) substrate and stopped after 20 min with 30  $\mu$ L of 1 M H<sub>2</sub>SO<sub>4</sub>. The absorbance was read at 450 nm by a Spectra photometer (Tecan Italia; Milan, Italy).

Mouse anti-PLTX 73D3 mAb was produced and purified from a hybridoma cell culture as previously described.<sup>29</sup>

**Hemolytic Assay.** In 96 multiwell plates, 125  $\mu$ L of toxin was added to wells containing 125  $\mu$ L of human red blood cells ( $10^8$  cells/ml in K<sup>+</sup>-free D-PBS) for 5 h at 37 °C. For negative controls, 125  $\mu$ L of red blood suspension were added to 125  $\mu$ L of K<sup>+</sup>-free D-PBS without toxin. The 100% of hemolysis (positive control) was given by 125  $\mu$ L of 0.1% Tween 20 (v/v). After 5 h, samples were centrifuged at 300g for 5 min to collect the supernatants. The absorbance of each supernatant was subsequently measured at 405/540 nm using a Spectra photometer (Tecan Italia; Milan, Italy).

**Indirect Sandwich ELISA.** The ELISA assay was carried out as previously described.<sup>29</sup> Briefly, multiwell strips coated with 100  $\mu$ L/well of mouse anti-PLTX 73D3 mAb (20  $\mu$ g/mL in PBS) and blocked with 200  $\mu$ L of 2% skimmed milk (w/v) dissolved in D-PBS containing 0.1% Tween 20 (PBS-Tw) were filled with toxins (100  $\mu$ L) diluted in PBS-Tw. After 2 h at room temperature (RT), 100  $\mu$ L of rabbit anti-PLTX polyclonal antibody (pAb) (0.17  $\mu$ g/mL) followed by 100  $\mu$ L of 1:2000 HRP-conjugated goat antirabbit pAb were added. After washes, 60  $\mu$ L of TMB were added to each well and the reaction stopped after 30 min with 30  $\mu$ L of H<sub>2</sub>SO<sub>4</sub> 1M. The absorbance was read at 450 nm (Spectra photometer; Tecan Italia; Milan, Italy).

Rabbit anti-PLTX pAb was produced after rabbit immunization with a bovine serum albumin-conjugated PLTX, as previously reported.<sup>29</sup>

**Statistical Analysis.** The effective concentration giving 50% of the maximal response (EC<sub>50</sub>) was calculated by a four-parameter curve-fitting nonlinear regression and K<sub>d</sub> constant by a one-site binding hyperbola nonlinear regression analysis using the GraphPad software, version 6.0 (Prism GraphPad, Inc.; San Diego, CA, USA); the statistical analysis was performed by *t* test (significant differences,  $p < 0.05$ ).

Concentration-effect curves of the different toxins were analyzed by a two-way ANOVA analysis followed by Bonferroni's post-test (PrismGraphPad, Inc.; San Diego, CA, USA) and significant differences were considered at  $p < 0.05$ .

Limit of detection (LOD), limit of quantitation (LOQ), and accuracy (Bias %) were calculated according to the international principles as described by Eurachem Guide.<sup>31</sup> LOD and LOQ were expressed as the analyte concentration corresponding to the average of 10 blank values plus 3 or 10 times the standard deviations, respectively. Accuracy was measured as % Bias over 10 replica, calculated as % difference between PLTX concentration measured by the assay and the theoretical

concentration in the sample divided by the theoretical concentration.

## RESULTS

### OVTX-a Cytotoxicity Is Lower than That of PLTX.

OVTX-a cytotoxicity was evaluated on HaCaT cells by MTT assay, after 4 h exposure to each toxin ( $10^{-16}$ – $10^{-7}$  M). Figure 2A shows the % of cell viability compared to negative controls (untreated cells). The concentration–effect curve of OVTX-a was compared to that of PLTX obtained under the same experimental conditions. OVTX-a reduced cell viability from the concentration of  $10^{-11}$  M ( $79.9 \pm 3.9\%$  cell viability) up to the concentration of  $10^{-8}$  M ( $5.4 \pm 1.3\%$  cell viability), with an  $EC_{50} = 1.1 \times 10^{-9}$  M (95% confidence interval, CI:  $0.7$ – $1.7 \times 10^{-9}$  M).

Exposure to PLTX induced a reduction of cell viability from the concentration of  $10^{-14}$  M ( $80.2 \pm 1.5\%$  cell viability) up to the concentration of  $10^{-8}$  M ( $5.8 \pm 0.7\%$  cell viability). The PLTX  $EC_{50}$  value was  $1.8 \times 10^{-11}$  M (95% CI:  $1.0$ – $3.4 \times 10^{-11}$  M), about 2 orders of magnitude lower than that of OVTX-a ( $p < 0.001$ ) (Figure 2A).

### OVTX-a Binding Affinity to HaCaT Cells Is Lower than That of PLTX.

To characterize OVTX-a binding to HaCaT cells, saturation experiments were performed exposing the intact cells to the toxin ( $5.1 \times 10^{-13}$ – $1.0 \times 10^{-8}$  M) for 10 min. Nonspecific binding was measured in the presence of  $1.0 \times 10^{-3}$  M OUA, added 10 min before OVTX-a. Figure 2B shows the saturation curves of the specific bindings of OVTX-a and PLTX obtained by subtracting the respective nonspecific bindings from the total ones. Regarding OVTX-a, a single binding site was found with a  $K_d$  value of  $1.2 \pm 0.4 \times 10^{-9}$  M, about 2 orders of magnitude higher ( $p < 0.001$ ) than that of PLTX ( $K_d = 2.7 \pm 0.6 \times 10^{-11}$  M).

### OVTX-a Hemolytic Activity Is Lower than That of PLTX.

The biological activity of OVTX-a was also evaluated using the human red blood cell hemolysis assay. As shown in Figure 3, hemolysis induced by OVTX-a was significantly lower

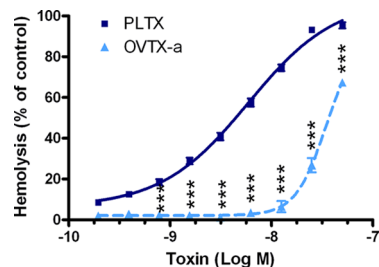


**Figure 3.** Hemolytic activity of OVTX-a. Human red blood cells were exposed to OVTX-a and PLTX ( $5.0 \times 10^{-8}$ – $1.9 \times 10^{-10}$  M) for 5 h at 37 °C. Results are reported as % of hemolysis with respect to the positive control (0.1% Tween 20) and are the means  $\pm$  SE of five different experiments performed in triplicate. Statistical differences: \*\*\*,  $p < 0.001$  (two-way ANOVA and Bonferroni's post test).

than that induced by PLTX, with an  $EC_{50}$  value of  $3.4 \times 10^{-8}$  M (95% CI:  $2.3$ – $5.1 \times 10^{-8}$  M), more than an order of magnitude higher ( $p < 0.001$ ) than that of the parent compound ( $EC_{50} = 5.9 \times 10^{-9}$  M; CI 95% =  $4.9$ – $7.2 \times 10^{-9}$  M).

**OVTX-a Is Detected by the ELISA Assay.** The ability of the sandwich ELISA recently developed for PLTX quantitation<sup>29</sup> to detect OVTX-a and a mixture of OVTXs (-a, -d, and

-e) was evaluated. The toxins were analyzed at concentrations within the working range of the sandwich ELISA for PLTX (1.3–80.0 ng/mL), and the obtained curves were compared to that of PLTX.

As shown in Figure 4A, both OVTX-a and the OVTXs mixture were detected in a concentration-dependent manner, similarly to PLTX: the  $EC_{50}$  values for OVTX-a (4.8 ng/mL; 95% CI: 4.3–5.3), OVTXs mixture (6.6 ng/mL; 95% CI: 4.6–9.7), and PLTX (4.3 ng/mL; 95% CI: 4.0–4.7 ng/mL) were comparable, with overlapping confidence intervals ( $p > 0.05$ ).

The calculated LOD and LOQ for OVTX-a were 4.2 and 5.6 ng/mL, respectively. The working range has been analyzed by linear regression, plotting the theoretical OVTX-a concentrations submitted to the analysis against toxin concentrations measured by the assay (Figure 4B), with a good correlation coefficient ( $r^2 = 0.9814$ ;  $n = 6$ ) and a good accuracy (Bias = 0.3%; range: –7.3 to 15.8%).

The ability of the sandwich ELISA to quantify OVTX-a in natural samples was then assessed. Eleven *Ostreopsis cf. ovata* extracts, nine *Ostreopsis cf. ovata* culture media and five mussel (*Mytilus galloprovincialis*) extracts containing OVTX-a at different concentrations (as assessed by LC-HRMS analysis) have been analyzed by the ELISA assay (Figure 4C,D,E). On the whole, the sandwich ELISA was able to quantify OVTX-a similarly to LC-HRMS ( $r^2 = 0.9540$ , 0.9849, and 0.9281 for *Ostreopsis* cells, *Ostreopsis* culture media, and mussels extracts, respectively).

### Ost-D Cytotoxicity and Detection by the ELISA Assay.

The cytotoxicity of Ost-D was evaluated for structure–activity relationship analysis. Ost-D cytotoxicity was evaluated on HaCaT cells by MTT assay after 4 h exposure to the toxin ( $10^{-16}$ – $10^{-7}$  M) and compared to that of PLTX (Figure 5A). Ost-D induced a reduction of cell viability from the concentration of  $10^{-14}$  M ( $83.2 \pm 2.9\%$  cell viability) up to the concentration of  $10^{-6}$  M ( $8.7 \pm 0.6\%$  cell viability), with an  $EC_{50} = 2.3 \times 10^{-8}$  M (95% CI:  $1.2$ – $4.4 \times 10^{-8}$  M), about 3 orders of magnitude higher than that of PLTX ( $p < 0.001$ ).

The sandwich ELISA was investigated also for Ost-D detection at concentrations within the working range for PLTX (1.3–80.0 ng/mL), and the obtained curve was compared to that of PLTX. As shown in Figure 5B, Ost-D was detected in a concentration-dependent manner by the sandwich ELISA, but considerably in lesser extent than PLTX. Indeed, the  $EC_{50}$  values for Ost-D and PLTX were equal to 40.6 ng/mL (95% CI: 38.0–43.4 ng/mL) and 4.3 ng/mL (95% CI: 4.0–4.7 ng/mL), respectively, being significantly different ( $p < 0.001$ ).

## DISCUSSION

Toxic benthic dinoflagellates of the genus *Ostreopsis* have been recognized for decades in tropical and subtropical regions. Only recently they have appeared in temperate areas, such as the Mediterranean Sea and NE Atlantic ocean.<sup>32</sup> In these areas cases of sanitary problems after skin contact and/or inhalational exposure to marine aerosol or direct contact with seawater during *Ostreopsis cf. ovata* blooms have been reported almost every year.<sup>4</sup> In the past few years, it has been proven that among PLTXs, OVTX-a is the major toxin produced by *Ostreopsis cf. ovata* in the Mediterranean Sea and high amounts of this toxin have been found in edible marine organisms all along the Mediterranean coasts.<sup>10,11,23,26</sup> In addition, *Ostreopsis cf. ovata* cells fragments were recently identified in marine aerosol along the Spanish coasts by qPCR assays<sup>33</sup> along with

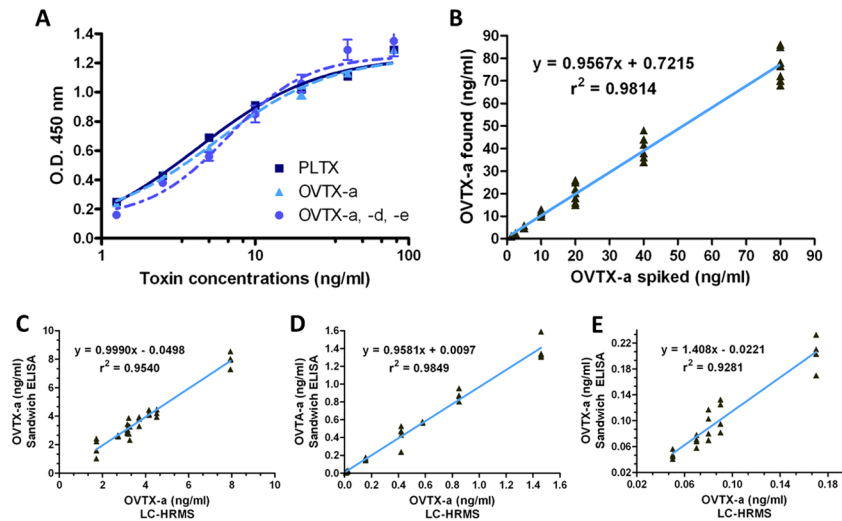


**Figure 4.** Detection of OVTX-a and a mixture of OVTX-a, -d, and -e by ELISA assay. (A) Calibration curve for OVTX-a and OVTXs mixture in comparison to that of PLTX. Each point represents the mean  $\pm$  SE of five different experiments performed in duplicate. (B) The working range of OVTX-a was analyzed by linear regression, plotting the theoretic OVTX-a concentrations against OVTX-a concentrations measured by the assay ( $n = 6$ ). (C) Detection of OVTX-a in *Ostreopsis cf. ovata* extracts ( $n = 11$ ), (D) in *Ostreopsis cf. ovata* culture media ( $n = 9$ ), and (E) in mussels (*Mytilus galloprovincialis*) extracts ( $n = 5$ ) containing OVTX-a (as assessed by LC-HRMS analysis). Results obtained by the sandwich ELISA were plotted against the quantification carried out by LC-HRMS and analyzed by linear regression.

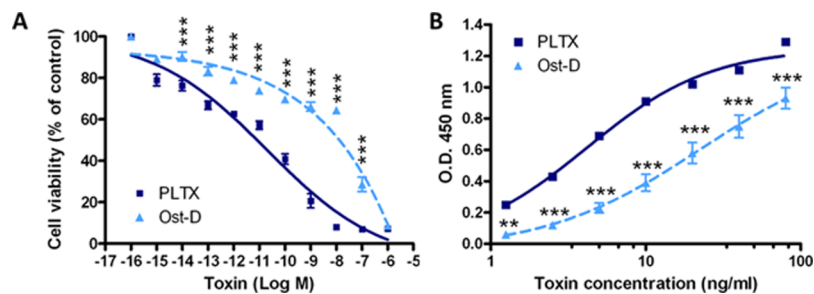


**Figure 5.** Cytotoxicity and detection of Ost-D. (A) Cells were exposed to Ost-D and PLTX ( $10^{-16}$ – $10^{-7}$  M) for 4 h, and cell viability evaluated by MTT assay. Results are reported as % of control. (B) Detection of Ost-D by ELISA assay compared to PLTX. Each point represents the mean  $\pm$  SE of five different experiments performed in duplicate. Statistical differences: \*,  $p < 0.05$ ; \*\*,  $p < 0.01$ ; \*\*\*,  $p < 0.001$  (Two-way ANOVA and Bonferroni's post test).

OVTXs that were detected directly in marine aerosols collected concomitantly with *O. cf. ovata* blooms along Tuscany (Italy) coasts.<sup>34</sup>

The detection of OVTX-a in *Ostreopsis* cells, seafood, and marine aerosols prompts the need to characterize its toxicological potential as well as to provide suitable detection methods for monitoring purposes. However, because limited amounts of purified toxin precluded animal studies, an in vitro approach was used.

Because no human cases of seafood poisoning ascribed to PLTXs have been recorded in these areas to date, but dermatotoxic effects are recurrently and commonly reported, OVTX-a was evaluated for its cytotoxicity on human HaCaT skin keratinocytes, a suitable cell model for the in vitro characterization of dermatotoxic agents<sup>35</sup> and one of the most sensitive cell line to PLTX.<sup>36–38</sup> The in vitro assay demonstrated, for the first time, that OVTX-a cytotoxicity is lower than that of PLTX, reducing cell viability with an  $EC_{50}$  ( $1.1 \times 10^{-9}$  M) about 2 orders of magnitude higher than that of PLTX ( $EC_{50} = 1.8 \times 10^{-11}$  M). This result is in perfect agreement with the reduced binding affinity of OVTX-a to HaCaT cells. Indeed, the  $K_d$  value of OVTX-a is about 2 orders of magnitude higher than that of PLTX. Moreover, the reduced

cytotoxicity of OVTX-a is confirmed by the reduced hemolytic activity. The latter result seems to be in disagreement with previous investigations reporting the same hemolytic activity for PLTX and OVTXs. However, these conclusions were achieved using *Ostreopsis* crude extracts containing a mixture of OVTXs and, in some cases, also traces of isobaric PLTX, among other compounds. These crude extracts may potentially contain other unidentified compounds that could tentatively be hemolytic, thus contributing to the total hemolytic effect.<sup>11,16</sup> However, since OVTX-a seems to be the major toxin produced by *Ostreopsis cf. ovata* in the Mediterranean Sea, these results, if confirmed by in vivo studies, could have a significant impact in the evaluation of the actual risk for human health associated with *Ostreopsis cf. ovata* in these areas.

Even though lower than that of PLTX, OVTX-a cytotoxicity falls in the nanomolar concentration range after an exposure time as short as 4 h, suggesting that this PLTX analog represents a real risk for human health after cutaneous exposure. In fact, several people have developed moderate to severe dermatitis after exposure to marine aerosols and/or accidental contact with *Ostreopsis cf. ovata* blooms. The severity of these exposures was sufficient to warrant treatment with steroidal and nonsteroidal anti-inflammatory drugs.

For this reason methods to detect OVTX-a are required. A sandwich ELISA has been recently developed to quantify PLTX in different matrices.<sup>29</sup> This simple ELISA assay was characterized for its ability to quantify OVTX-a as well as an OVTX mixture (OVTX-a, -d, and -e). These analogues are detected by the sandwich ELISA in an overlapping manner in comparison to PLTX. Moreover, the assay is sensitive (LOD and LOQ of 4.2 and 5.6 ng/mL, respectively) and accurate (Bias of 0.3%). This could suggest a good efficiency in the quantitation of OVTX-a also in contaminated natural samples. Indeed, the ELISA quantitation of OVTX-a in contaminated samples is comparable to that of LC-HRMS. In a total of 25 contaminated natural samples (11 *Ostreopsis cf. ovata*, 9 *Ostreopsis cf. ovata* cell culture media, and 5 *Mytilus galloprovincialis* extracts) submitted for analyses, OVTX-a was quantified in a similar manner with respect to that quantified by LC-HRMS, as shown by the high  $r^2$  values. These data suggest an excellent applicability of the sandwich ELISA for OVTX-a quantitation in complex biological samples of marine origin.

Interestingly, two *Ostreopsis cf. ovata* cell extracts, not containing PLTXs by LC-HRMS analysis, were negative also in the ELISA analysis, suggesting the specificity of the assay in the quantitation of PLTXs.

On the contrary, the ELISA assay detected Ost-D to a lower extent than PLTX. However, Ost-D has been detected in Japanese strains of *O. siamensis*, while Mediterranean/Atlantic strains of *O. cf. siamensis* have been found to be devoid of any appreciable toxin content.<sup>39,40</sup> In addition, the ability of the assay to quantify not only OVTX-a but also a mixture of OVTXs, in an overlapping manner, highlights its applicability in a real-life situation, in which mussels are likely to be contaminated by a mixture of OVTXs rather than by OVTX-a alone. Thus, the ELISA assay could be used as a screening method to detect OVTXs, before confirmatory analysis by LC-HRMS. This could be particularly important and helpful at the beginning of an *Ostreopsis cf. ovata* bloom, since the presence of OVTXs could be confirmed within some hours, allowing time to issue an alert to avoid sanitary problems but also economic losses to the tourism industry due to possible false alarmism. Previously, using the same monoclonal antibodies employed in the sandwich ELISA, we proposed an immunocytochemical assay directly on *Ostreopsis cf. ovata* cells, which is much more complicated, costly and time-consuming.<sup>41</sup>

Intriguingly, the presented data suggests that even small changes in the complex PLTX molecular structure, such as three missing hydroxy groups on C17, C44, and C64, one additional hydroxy group on C42, and a configurational inversion at C26 in OVTX-a (Figure 1), significantly reduce its toxicity with respect to PLTX. So far, it is only known that the N-terminal portion is required for PLTX toxicity, possibly allowing the dimerization of the toxin.<sup>42</sup> To investigate the structural features necessary for the PLTX cytotoxic effect, data regarding PLTX and OVTX-a have been compared to those obtained exposing HaCaT cells to Ost-D (a 42-OH-PLTX lacking two hydroxy groups on C19 and C44 and two methyl groups on C3 and C26). Compared to PLTX, the common features between OVTX-a and Ost-D are an additional hydroxyl group on C42 and a missing hydroxyl group on C44. On the other hand, compared to PLTX, OVTX-a lacks the hydroxyl group at C17, while Ost-D lacks the hydroxyl group at C19. Cell viability reduction by Ost-D was 3 orders of magnitude lower than that induced by PLTX and 1 order of magnitude lower than that induced by OVTX-a, with an order

of potencies of PLTX > OVTX-a > Ost-D. This allows us to make some observations regarding the relationship between the structure and cytotoxic activity of these toxins: (i) the additional hydroxyl group at C42 seems not to be important for the cytotoxic effect since 42-OH-PLTX and PLTX show similar cytotoxicities<sup>6,8</sup> (ii) the missing hydroxyl group on C44, a common feature between OVTX-a and Ost-D, but present in PLTX and 42-OH-PLTX, seems to be determinant for PLTX cytotoxic activity since both of them are largely less toxic than the parent compound; (iii) the missing methyl and hydroxy groups at C3, C19 and C26 of Ost-D, in comparison to OVTX-a, could further reduce the toxin cytotoxicity. However, we cannot exclude that other factors such as hydroxyl group lacking at C17 or at C19, stereochemical changes, and consequent conformational changes, could affect the total cytotoxic activity.

In conclusion, this study provides the first characterization of the cytotoxic effects of OVTX-a. In particular, OVTX-a appears to be less toxic in vitro compared to the reference compound PLTX, displaying lower binding affinity and cytotoxicity on HaCaT cells as well as a lower hemolytic activity on human erythrocytes. Structure–activity considerations suggest that the lack of a hydroxy group at C44 is determinant for PLTX cytotoxicity. Despite OVTX-a cytotoxicity is lower than that of PLTX, it is exerted at nanomolar concentrations after a short exposure time, suggesting that OVTX-a is a legitimate concern for human health. The sandwich ELISA for PLTX detection can also quantify OVTX-a in contaminated marine samples suggesting that it can be a simple method for self-monitoring by shellfish producers as well as monitoring programs for the detection of *Ostreopsis cf. ovata* toxins.

## ■ AUTHOR INFORMATION

### Corresponding Author

\*Address: Department of Life Sciences, University of Trieste, Via A. Valerio 6, 34127 Trieste, Italy; e-mail: [tubaro@units.it](mailto:tubaro@units.it); tel.: +39.040.5588835; fax: +39.040.5583165.

### Notes

The authors declare no competing financial interest.

## ■ ACKNOWLEDGMENTS

This work was supported by a grant of the University of Trieste (Università degli Studi di Trieste - Finanziamento di Ateneo per progetti di ricerca scientifica - FRA 2012). Chemical analyses were carried out in the framework of Programme STAR Linea 1 2013 (VALTOX, Napoli\_call2013\_08) financially supported by University of Naples and Compagnia di San Paolo. The authors are grateful to Prof. Takeshi Yasumoto (Japan Food Research Laboratories) for kindly supply ostreocin-D.

## ■ REFERENCES

(1) Moore, R. E.; Scheuer, P. J. Palytoxin: A new marine toxin from a coelenterate. *Science* **1971**, *172*, 495–498.

- (2) Moore, R. E.; Helfrich, P.; Patterson, G. M. L. The deadly seaweed of Hana. *Oceanus* **1982**, *25*, 54–63.
- (3) Ciminiello, P.; Dell'Aversano, C.; Fattorusso, E.; Forino, M.; Magno, G. S.; Tartaglione, L.; Grillo, C.; Melchiorre, N. The Genoa 2005 outbreak. Determination of putative palytoxin in Mediterranean *Ostreopsis ovata* by a new liquid chromatography tandem mass spectrometry method. *Anal. Chem.* **2006**, *78*, 6153–6159.
- (4) Tubaro, A.; Durando, P.; Del Favero, G.; Ansaldi, F.; Icardi, G.; Deeds, J. R.; Sosa, S. Case definitions for human poisonings postulated to palytoxins exposure. *Toxicol.* **2011**, *57*, 478–495.
- (5) Kerbrat, A. S.; Amzil, Z.; Pawlowicz, R.; Golubic, S.; Sibat, M.; Darius, H. T.; Chinain, M.; Laurent, D. First evidence of palytoxin and 42-hydroxy-palytoxin in the marine cyanobacterium *Trichodesmium*. *Mar. Drugs* **2011**, *9*, 543–560.
- (6) Ciminiello, P.; Dell'Aversano, C.; Dello Iacovo, E.; Fattorusso, E.; Forino, M.; Grauso, L.; Tartaglione, L.; Florio, C.; Lorenzon, P.; De Bortoli, M.; Tubaro, A.; Poli, M.; Bignami, G. Stereostructure and biological activity of 42-hydroxy-palytoxin: a new palytoxin analogue from Hawaiian *Palythoa* subspecies. *Chem. Res. Toxicol.* **2009**, *22*, 1851–1859.
- (7) Tubaro, A.; Del Favero, G.; Beltramo, D.; Ardizzone, M.; Forino, M.; De Bortoli, M.; Pelin, M.; Poli, M.; Bignami, G.; Ciminiello, P.; Sosa, S. Acute oral toxicity in mice of a new palytoxin analog: 42-hydroxy-palytoxin. *Toxicol.* **2011**, *57*, 755–763.
- (8) Ciminiello, P.; Dell'Aversano, C.; Dello Iacovo, E.; Forino, M.; Tartaglione, L.; Pelin, M.; Sosa, S.; Tubaro, A.; Chaloin, O.; Poli, M.; Bignami, G. Stereoisomers of 42-hydroxy palytoxin from hawaiian *Palythoa toxica* and *P. tuberculosa*: stereostructure elucidation, detection, and biological activities. *J. Nat. Prod.* **2014**, *77*, 351–357.
- (9) Ito, E.; Yasumoto, T. Toxicological studies on palytoxin and ostreocin-D administered to mice by three different routes. *Toxicol.* **2009**, *54*, 244–251.
- (10) Ciminiello, P.; Dell'Aversano, C.; Dello Iacovo, E.; Fattorusso, E.; Forino, M.; Grauso, L.; Tartaglione, L.; Guerrini, F.; Pezzolesi, L.; Pistocchi, R.; Vanucci, S. Isolation and structure elucidation of ovatoxin-a, the major toxin produced by *Ostreopsis ovata*. *J. Am. Chem. Soc.* **2012**, *134*, 1869–1875.
- (11) Brissard, C.; Herrenknecht, C.; Séchet, V.; Hervé, F.; Pisapia, F.; Harcouet, J.; Lémée, R.; Chomérat, N.; Hess, P.; Amzil, Z. Complex toxin profile of French Mediterranean *Ostreopsis cf. ovata* strains, seafood accumulation and ovatoxins prepurification. *Mar. Drugs* **2014**, *12*, 2851–2876.
- (12) García-Altres, M.; Tartaglione, L.; Dell'Aversano, C.; Carnicer, O.; de la Iglesia, P.; Forino, M.; Diogène, J.; Ciminiello, P. The novel ovatoxin-g and isobaric palytoxin (so far referred to as putative palytoxin) from *Ostreopsis cf. ovata* (NW Mediterranean Sea): structural insights by LC-high resolution MS(n). *Anal. Bioanal. Chem.* **2015**, *407*, 1191–1204.
- (13) Patocka, J.; Gupta, R. C.; Wu, Q. H.; Kuca, K. Toxic potential of palytoxin. *J. Huazhong Univ. Sci. Technol., Med. Sci.* **2015**, *35*, 773–780.
- (14) Amzil, Z.; Sibat, M.; Chomérat, N.; Gossel, H.; Marco-Miralles, F.; Lemee, R.; Nezan, E.; Sechet, V. Ovatoxin-a and palytoxin accumulation in seafood in relation to *Ostreopsis cf. ovata* blooms on the french mediterranean coast. *Mar. Drugs* **2012**, *10*, 477–496.
- (15) Ciminiello, P.; Dell'Aversano, C.; Dello Iacovo, E.; Forino, M.; Tartaglione, L. Liquid chromatography-high-resolution mass spectrometry for palytoxins in mussels. *Anal. Bioanal. Chem.* **2015**, *407*, 1463–1473.
- (16) Pezzolesi, L.; Guerrini, F.; Ciminiello, P.; Dell'Aversano, C.; Dello Iacovo, E.; Fattorusso, E.; Forino, M.; Tartaglione, L.; Pistocchi, R. Influence of temperature and salinity on *Ostreopsis cf. ovata* growth and evaluation of toxin content through HR LC-MS and biological assays. *Water Res.* **2012**, *46*, 82–92.
- (17) Crinelli, R.; Carloni, E.; Giacomini, E.; Penna, A.; Dominici, S.; Battocchi, C.; Ciminiello, P.; Dell'Aversano, C.; Fattorusso, E.; Forino, M.; Tartaglione, L.; Magnani, M. Palytoxin and an *Ostreopsis* toxin extract increase the levels of mRNAs encoding inflammation-related proteins in human macrophages via p38 mapk and nf-kappab. *PLoS One* **2012**, *7*, e38139.
- (18) Pagliara, P.; Scarano, A.; Barca, A.; Zuppone, S.; Verri, T.; Caroppo, C. *Ostreopsis cf. ovata* induces cytoskeletal disorganization, apoptosis, and gene expression dysregulation on hela cells. *J. Appl. Phycol.* **2015**, *27*, 2321–2332.
- (19) Gorbi, S.; Avio, G. C.; Benedetti, M.; Totti, C.; Accoroni, S.; Pichierri, S.; Bacchiocchi, S.; Orletti, R.; Graziosi, T.; Regoli, F. Effects of harmful dinoflagellate *Ostreopsis cf. ovata* exposure on immunological, histological and oxidative responses of mussels *Mytilus galloprovincialis*. *Fish Shellfish Immunol.* **2013**, *35*, 941–950.
- (20) Faimali, M.; Giussani, V.; Piazza, V.; Garaventa, F.; Corra, C.; Asnaghi, V.; Privitera, D.; Gallus, L.; Cattaneo-Vietti, R.; Mangialajo, L.; Chiantore, M. Toxic effects of harmful benthic dinoflagellate *Ostreopsis ovata* on invertebrate and vertebrate marine organisms. *Mar. Environ. Res.* **2012**, *76*, 97–107.
- (21) Pagliara, P.; Caroppo, C. Toxicity assessment of *Amphidinium carterae*, *Coolia* cfr. *monotis* and *Ostreopsis* cfr. *ovata* (dinophyta) isolated from the northern ionian sea (mediterranean sea). *Toxicol.* **2012**, *60*, 1203–1214.
- (22) Ciminiello, P.; Dell'Aversano, C.; Fattorusso, E.; Forino, M.; Tartaglione, L.; Grillo, C.; Melchiorre, N. Putative palytoxin and its new analogue, ovatoxin-a, in *Ostreopsis ovata* collected along the Ligurian coasts during the 2006 toxic outbreak. *J. Am. Soc. Mass Spectrom.* **2008**, *19*, 111–120.
- (23) Ciminiello, P.; Dell'Aversano, C.; Dello Iacovo, E.; Forino, M.; Tartaglione, L. Liquid chromatography-high resolution mass spectrometry for palytoxins in mussels. *Anal. Bioanal. Chem.* **2015**, *407*, 1463–1473.
- (24) Durando, P.; Ansaldi, F.; Oreste, P.; Moscatelli, P.; Marensi, L.; Grillo, C.; Gasparini, R.; Icardi, G. *Ostreopsis ovata* and human health: epidemiological and clinical features of respiratory syndrome outbreaks from a two year syndromic surveillance, 2005–2006, in northwest Italy. *Euro Surveill.* **2007**, *12*, E070607.1.
- (25) Kermarec, F.; Dor, F.; Armengaud, A.; Charlet, F.; Kantin, R.; Sauzade, D.; de Haro, L. Health risks related to *Ostreopsis ovata* in recreational waters. *Env. Risques Santé.* **2008**, *7*, 357–363.
- (26) Tichadou, L.; Glaizal, M.; Armengaud, A.; Gossel, H.; Lemée, R.; Kantin, R.; Lasalle, J. L.; Drouet, G.; Rambaud, L.; Malfait, P.; de Haro, L. Health impact of unicellular algae of the *Ostreopsis* genus blooms in the Mediterranean Sea: experience of the French Mediterranean coast surveillance network from 2006 to 2009. *Clin. Toxicol.* **2010**, *48*, 839–844.
- (27) Ukena, T.; Satake, M.; Usami, M.; Oshima, Y.; Naoki, H.; Fujita, T.; Kan, Y.; Yasumoto, T. Structure elucidation of ostreocin-d, a palytoxin analog isolated from the dinoflagellate *ostreopsis siamensis*. *Biosci., Biotechnol., Biochem.* **2001**, *65*, 2585–2588.
- (28) Hoshaw, R. W.; Rosowski, J. R. Methods for microscopic algae. In *Handbook of Phycological Methods*; Stein, J. R., Ed.; Cambridge University Press: New York, 1973; pp 53–67.
- (29) Boscolo, S.; Pelin, M.; De Bortoli, M.; Fontanive, G.; Barreras, A.; Berti, F.; Sosa, S.; Chaloin, O.; Bianco, A.; Yasumoto, T.; Prato, M.; Poli, M.; Tubaro, A. Sandwich ELISA assay for the quantitation of palytoxin and its analogs in natural samples. *Environ. Sci. Technol.* **2013**, *47*, 2034–2042.
- (30) Pelin, M.; Boscolo, S.; Poli, M.; Sosa, S.; Tubaro, A.; Florio, C. Characterization of palytoxin binding to HaCaT cells using a monoclonal anti-palytoxin antibody. *Mar. Drugs* **2013**, *11*, 584–598.
- (31) EC (European Commission) Commission decision of 15 March 2002 laying down detailed rules for the implementation of Council Directive 91/492/ECC as regards the maximum levels and the methods of analysis of certain marine biotoxins in bivalve molluscs, echinoderms, tunicates and marine gastropods (2002/225/EC). *Off. J. Eur. Commun.* **2002**, *175*, 62–64.
- (32) David, H.; Moita, M. T.; Laza-Martínez, A.; Silva, A.; Mateus, M.; Pablo, H.; Orive, E. First bloom of *Ostreopsis cf. ovata* in the continental Portuguese coast. *Harmful Algae News* **2012**, *45*, 12–13.
- (33) Casabianca, S.; Casabianca, A.; Riobó, P.; Franco, J. M.; Vila, M.; Penna, A. Quantification of the toxic dinoflagellate *Ostreopsis* spp. by qPCR assay in marine aerosol. *Environ. Sci. Technol.* **2013**, *47*, 3788–3795.

- (34) Ciminiello, P.; Dell'Aversano, C.; Dello Iacovo, E.; Fattorusso, E.; Forino, M.; Tartaglione, L.; Benedettini, G.; Onorari, M.; Serena, F.; Battocchi, C.; Casabianca, S.; Penna, A. First finding of *Ostreopsis* cf. *ovata* toxins in marine aerosols. *Environ. Sci. Technol.* **2014**, *48*, 3532–3540.
- (35) Boukamp, P.; Petrussevska, R. T.; Breitkreutz, D.; Hornung, J.; Markham, A.; Fusenig, N. E. Normal keratinization in a spontaneously immortalized aneuploid human keratinocyte cell line. *J. Cell Biol.* **1988**, *106*, 761–771.
- (36) Pelin, M.; Zanette, C.; De Bortoli, M.; Sosa, S.; Della Loggia, R.; Tubaro, A.; Florio, C. Effects of the marine toxin palytoxin on human skin keratinocytes: role of ionic imbalance. *Toxicology* **2011**, *282*, 30–38.
- (37) Pelin, M.; Ponti, C.; Sosa, S.; Gibellini, D.; Florio, C.; Tubaro, A. Oxidative stress induced by palytoxin in human keratinocytes is mediated by a H<sup>+</sup>-dependent mitochondrial pathway. *Toxicol. Appl. Pharmacol.* **2013**, *266*, 1–8.
- (38) Pelin, M.; Sosa, S.; Pacor, S.; Tubaro, A.; Florio, C. The marine toxin palytoxin induces necrotic death in HaCaT cells through a rapid mitochondrial damage. *Toxicol. Lett.* **2014**, *229*, 440–450.
- (39) Ciminiello, P.; Dell'Aversano, C.; Dello Iacovo, E.; Fattorusso, E.; Forino, M.; Tartaglione, L.; Yasumoto, T.; Battocchi, C.; Giacobbe, M.; Amorim, A.; Penna, A. Investigation of toxin profile of Mediterranean and Atlantic strains of *Ostreopsis* cf. *siamensis* (Dinophyceae) by liquid chromatography–high resolution mass spectrometry. *Harmful Algae* **2013**, *23*, 19–27.
- (40) Parsons, M. L.; Aligizaki, K.; Bottein, M. Y. D.; Fraga, S.; Morton, S. L.; Penna, A.; Rhodes, L. *Gambierdiscus* and *Ostreopsis*: reassessment of the state of knowledge of their taxonomy, geography, ecophysiology, and toxicology. *Harmful Algae* **2012**, *14*, 107–129.
- (41) Honsell, G.; De Bortoli, M.; Boscolo, S.; Dell'Aversano, C.; Battocchi, C.; Fontanive, G.; Penna, A.; Berti, F.; Sosa, S.; Yasumoto, T.; Ciminiello, P.; Poli, M.; Tubaro, A. Harmful dinoflagellate *Ostreopsis* cf. *ovata* Fukuyo: detection of ovatoxins in field samples and cell immunolocalization using antipalytoxin antibodies. *Environ. Sci. Technol.* **2011**, *45*, 7051–7059.
- (42) Inuzuka, T.; Uemura, D.; Arimoto, H. The conformation features of palytoxin in aqueous solution. *Tetrahedron* **2008**, *64*, 7718–7723.